



International Institute for
Applied Systems Analysis
www.iiasa.ac.at

Reference, Preference, Convexity and Efficiency - Basic Notions in Multiobjective Decision Making

Peschel, M., Ester, J. & Nguyen, T.L.

IIASA Working Paper

WP-80-002

January 1980



Peschel M, Ester J, & Nguyen TL (1980). Reference, Preference, Convexity and Efficiency - Basic Notions in Multiobjective Decision Making. IIASA Working Paper. IIASA, Laxenburg, Austria: WP-80-002 Copyright © 1980 by the author(s). <http://pure.iiasa.ac.at/id/eprint/1467/>

Working Papers on work of the International Institute for Applied Systems Analysis receive only limited review. Views or opinions expressed herein do not necessarily represent those of the Institute, its National Member Organizations, or other organizations supporting the work. All rights reserved. Permission to make digital or hard copies of all or part of this work for personal or classroom use is granted without fee provided that copies are not made or distributed for profit or commercial advantage. All copies must bear this notice and the full citation on the first page. For other purposes, to republish, to post on servers or to redistribute to lists, permission must be sought by contacting repository@iiasa.ac.at

NOT FOR QUOTATION
WITHOUT PERMISSION
OF THE AUTHOR

REFERENCE, PREFERENCE, CONVEXITY
AND EFFICIENCY--BASIC NOTIONS IN
MULTIOBJECTIVE DECISION MAKING

M. Peschel
J. Ester
Nguyen Thuc Loan

January 1980
WP-80-2

Working Papers are interim reports on work of the International Institute for Applied Systems Analysis and have received only limited review. Views or opinions expressed herein do not necessarily represent those of the Institute or of its National Member Organizations.

INTERNATIONAL INSTITUTE FOR APPLIED SYSTEMS ANALYSIS
A-2361 Laxenburg, Austria

M. Peschel is with the Academy of Sciences of the GDR, Berlin.

J. Ester is with the Technical High School of Karl-Marx-Stadt, GDR.

Nguyen Thuc Loan is with the Center of Sciences, Hanoi, Vietnam.

PREFACE

In commonly used Pareto optimality the notions reference, preference, convexity and efficiency are interrelated and of great importance. It is shown that the usual notion of convexity on the base of straight lines is not consistent with Pareto optimality. There are many possibilities to reach all efficient points by using a parametrized set of compromise criteria.

Especially important for the decision maker's goal is to describe local wishes by corresponding reference points. It is useful to describe these reference points by preference levels or local utility fields. The method of direction diagrams helps to introduce the decision maker's imagination. The penalty scalarization method proves as a special case of direction diagrams. Direction diagrams serve for the design of good seeking procedures for efficient points expressed in terms of the control space.

REFERENCE, PREFERENCE, CONVEXITY
AND EFFICIENCY--
BASIC NOTIONS IN MULTIOBJECTIVE
DECISION MAKING

M. Peschel, J. Ester, Nguyen Thuc Loan

INTRODUCTION

We first interpret the basic notions reference, preference, convexity and efficiency for the well-known Pareto optimality. From this exercise we try to find generalizations, taking into account the local or global utility imagination of the decision maker. We restrict ourselves to a two-dimensional objective space, although most of our consideration can easily be extended to a finite-dimensional objective space.

The main technical tool used to construct fields for local utility is the direction diagram; these diagrams reflect the independent influences of the distance r and the angle ϕ of the reference vector between the point under consideration and a chosen reference point.

With direction diagrams we can interpret Pareto preferences as well as Wierzbicki's penalty scalarization method and construct many order-preserving local utility fields. This is important in order to reflect the changing goals of the decision maker. However, utility fields can also be used as models in the control space and the information they provide can be used to find qualified seeking procedures for the efficient points. Without reduction of generality we seek to maximize all our objectives.

PREFERENCE, REFERENCE, EFFICIENTY, AND CONVEXITY IN THE SENSE OF PARETO OPTIMALITY

We assume that we are dealing with two objectives Q_1, Q_2 that are dependent on a set of control variables a_1, a_2, \dots, a_k . Very often the relationship between the objectives Q_i and the controls a_j is a static vector function

$$Q_i = f_i(a_1, a_2, \dots, a_k) \quad i = 1, 2 \quad ,$$

with some appropriate demands at the functions f_i , such as differentiability. For simplicity let us assume $k = 2$, where the model $Q = f(a)$ is a mapping from a two-dimensional control space into a two-dimensional objective space. This vector function has a certain definition area A . All controls $a \in A$ are called feasible controls. The corresponding points $Q \in \Omega$ in the objective space are called feasible objectives or feasible goals. In a control space we represent the relationship $Q = f(a)$ by the fields of isolines of Q_1 and Q_2 separately, as shown in Figure 1. In an objective space we prefer to show the area Ω of all feasible goals that can have a form like that shown in Figure 2. In Pareto preference, a goal Q' is better than a goal Q :

$$Q' > Q \quad ,$$

if $Q'_i \geq Q_i$ and there exists at least one i_0 with $Q'_{i_0} > Q_{i_0}$.

There is a priori no differentiation between different goals Q belonging to the same preference class: better, worse, indifferent, which are shown in Figure 3 for an arbitrary reference point.

An efficient point in Pareto optimality is a maximum point (feasible) in the sense of vector halforder: Q^* efficient, if there is no feasible point Q' with $Q' > Q^*$. The set of all efficient points is called the Pareto set.

Figure 2 shows an example of a Pareto set. We learn from it, that the Pareto set can be disconnected, can contain isolated points and can have convex and concave parts. An attempt can be

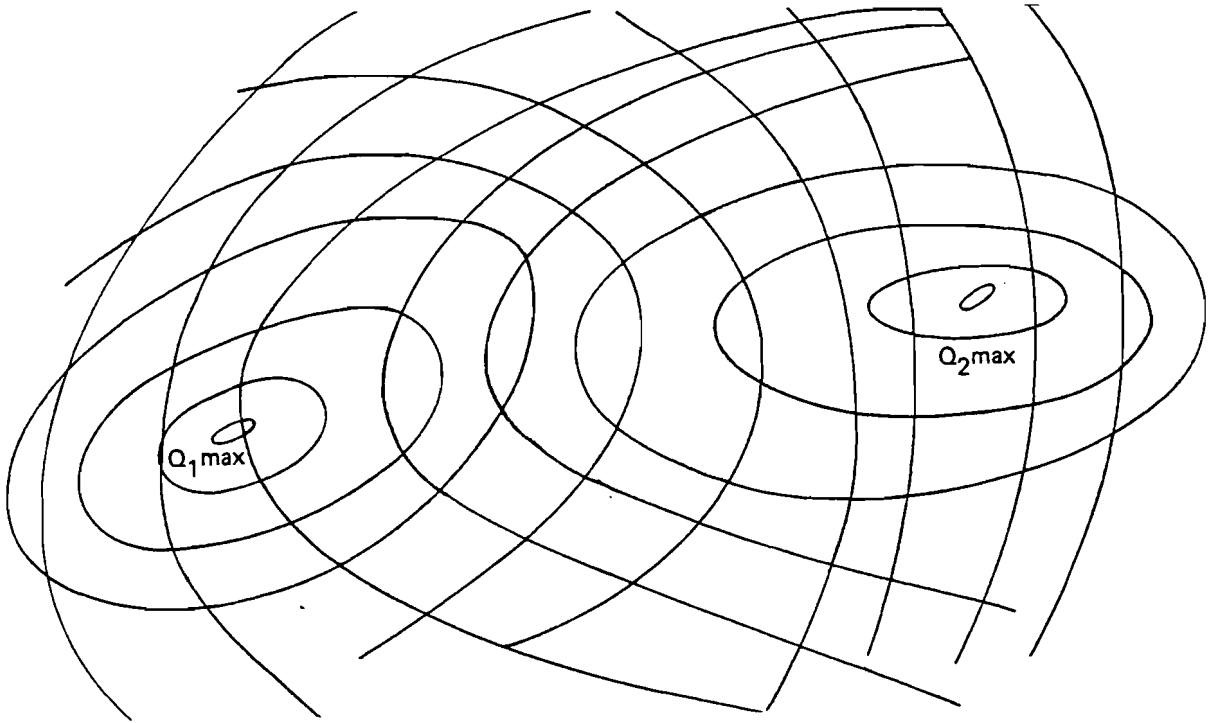


Figure 1: Level lines for different criteria

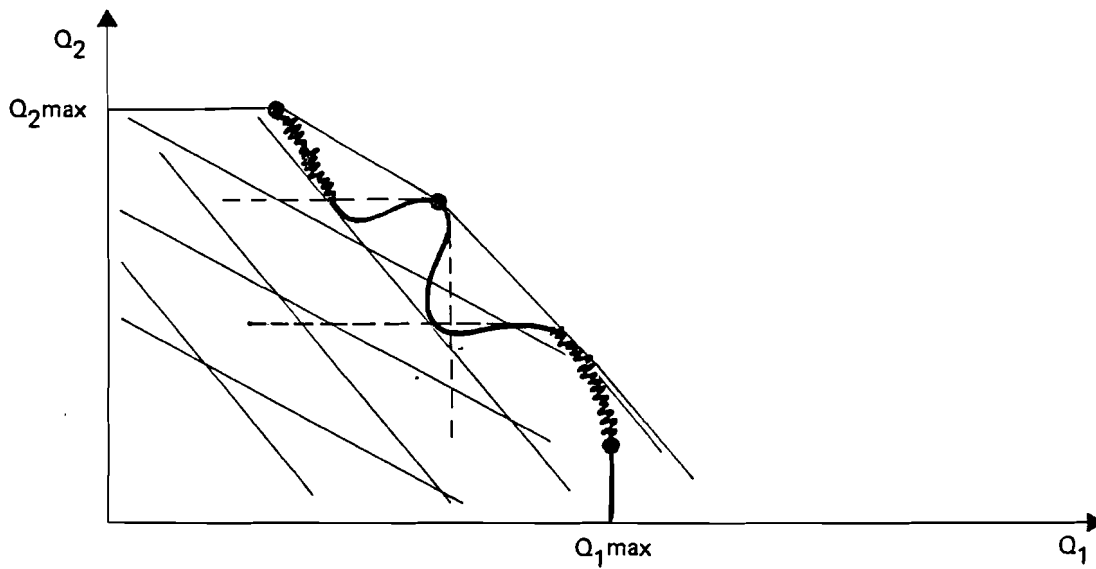


Figure 2: Example of a non-connected Pareto set with an isolated efficient point

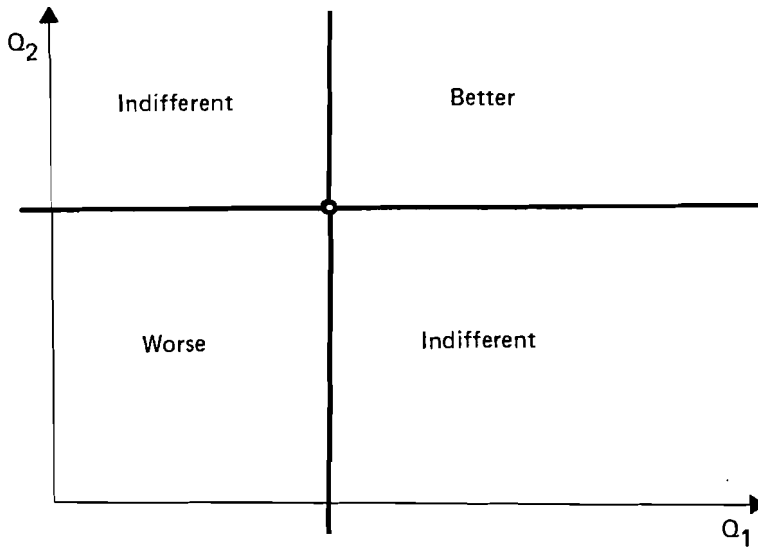


Figure 3: The preference areas in Pareto-optimality

made to find the efficient points by using weighting coefficients and linear compromises between the objectives--i.e., by applying global criteria of the form

$$\tilde{Q} = \lambda_1 Q_1 + \lambda_2 Q_2, \quad \lambda_i \geq 0.$$

Figure 2 also shows that with this approach we can only reach those efficient points which belong to the convex hull of the feasible goal set Ω . The reason for this property is that the common notion of convexity is not consistent with Pareto optimality or expressed otherwise: Pareto optimality needs a corresponding notion of convexity.

The common convexity is based on straight lines. A set B is called convex if it contains with any two points $Q_1 \in B$, $Q_2 \in B$ all points on the linear segment

$$\lambda Q_1 + (1-\lambda)Q_2, \quad 0 \leq \lambda \leq 1.$$

Figure 4 shows examples for convex and nonconvex sets.

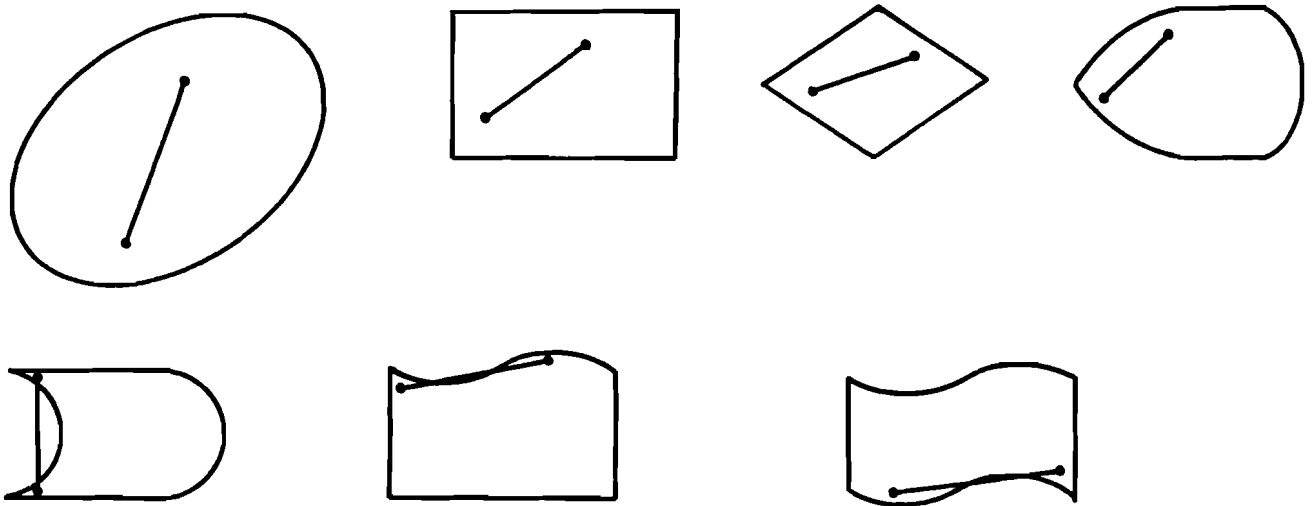


Figure 4: Some examples of convex and nonconvex sets in the sense of common convexity

Now we introduce convexity notions consistent with Pareto optimality.

Maximum Convexity [1]

Instead of straight lines we use lines parallel to the coordinate axes and angles to the left formed from them as shown in Figure 5.

Minimum Convexity [1]

Instead of straight lines we use lines parallel to the coordinate axes and angles to the right formed from them as shown in Figure 6. For every two points Q_1, Q_2 the "segment" Q_1Q_2 is uniquely determined although there is not necessarily only one "straight line" connecting them.

Figure 7 shows a convex set in maximum convexity and Figure 8 a convex set in minimum convexity. In Figure 7 the interesting convex set lies "southwest" of the boundary, while that in Figure 8 lies "northeast" of the boundary. Obviously in both cases straight lines do not support these sets, but rather the

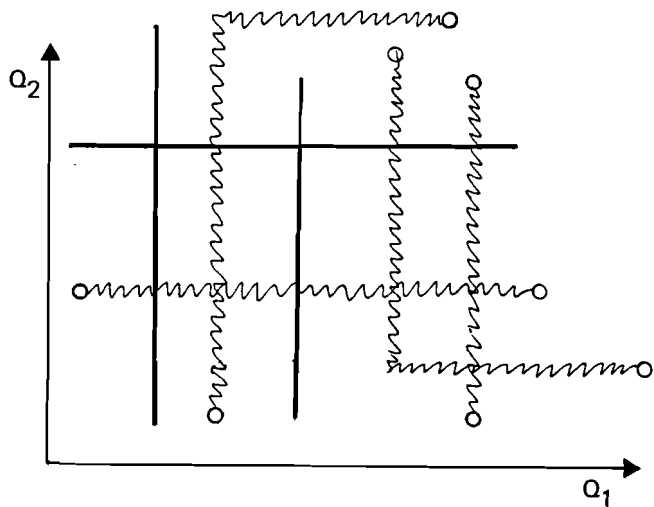


Figure 5: New "Straight Lines" in maximum convexity

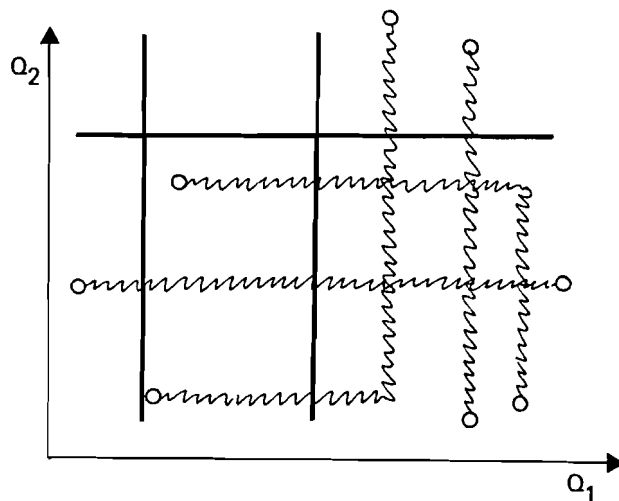


Figure 6: New "Straight Lines" in minimum convexity

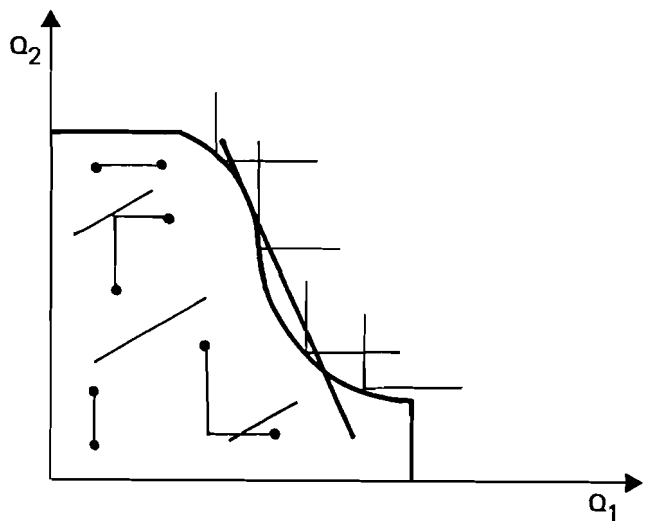


Figure 7: Example of a maximum convex set together with supporting "Straight Lines"

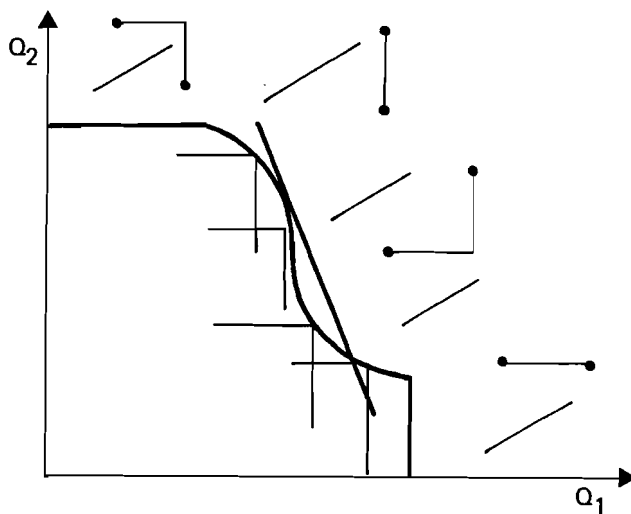


Figure 8: Example of a minimum convex set together with supporting "Straight Lines"

"straight lines" of the corresponding new convexity notion. The most important property for our aims is that shown in Figures 7 and 8.

The whole boundary without parts parallel to the coordinate axes in Figure 7 consists of the efficient points of a maximum problem, whereas in Figure 8 the corresponding boundary consists of efficient points of a minimum problem. This leads to an Efficiency theorem: In every efficient point of a vector maximum (minimum) problem there exists a supporting straight line of maximum (minimum) convexity.

Returning to the example in Figure 2, we explore the following result: The convex hull of a set contrasts the whole set of efficient points on the boundary. This is in contrast to the case where we form the common convex hull.

Finally we can see from Figures 7 and 8 that the following holds.

Duality theorem: If a set B is convex, in the sense of maximum convexity, its complement \bar{B} is convex in the sense of minimum convexity.

Let us now introduce fields of indifference lines to reach efficient points by optimizing suitable compromising criteria. We now consider the left lower angles \angle as indifference curves for vector maximum problems and the right upper angles \rceil as indifference curves for vector minimum problems. In fact this is not exactly true in Pareto optimality because only the corner points are indifferent; however a very small variation of these angles would lead to indifference curves \angle and \rceil respectively. Because of this duality we restrict the following considerations to the left lower angles. In the whole plane (Q_1, Q_2) we have such an angle, through every point, i.e., the whole set can be described by two parameters. We are now trying to enumerate otherwise all the angles following the idea, by using one parameter for the description of the efficient set and the other as a value of a compromising objective to find the corresponding efficient points. This can be done in the following way:

We choose in the plane (Q_1, Q_2) a field

$$Q_i = g_i(\lambda, \tilde{Q}) \quad i = 1, 2 \quad ,$$

of non-decreasing curves, i.e., only one of these curves goes through a given point Q^* of the plane. The parameter λ enumerates the various curves, and \tilde{Q} is the corresponding curve parameter. \tilde{Q} is chosen in such a way that for

$$\tilde{Q}_1 > \tilde{Q}_2 \quad ,$$

it follows that

$$g(\lambda, \tilde{Q}_1) \geq g(\lambda, \tilde{Q}_2) \quad ,$$

and conversely. Thus \tilde{Q} considered along a curve λ is order preserving.

Figure 9 presents some examples of this enumeration approach, always with the same vector maximization problem.

We now have another form of the Efficiency theorem: Every efficient maximum point can be determined by maximization of a global compromise criterion \tilde{Q} by choosing a certain value λ of the weighting parameter.

Under our assumptions the equations

$$Q_i = g_i(\lambda, \tilde{Q}) \quad i = 1, 2 \quad ,$$

can be solved uniquely after λ, \tilde{Q} and we get

$$\lambda = \rho(Q_1, Q_2) \quad ,$$

$$\tilde{Q} = \psi(Q_1, Q_2) \quad .$$

We can then formulate an equivalent Efficiency theorem: Every efficient maximum point can be reached by

$$\max_{Q_1, Q_2} \psi(Q_1, Q_2) | \rho(Q_1, Q_2) = \text{const.}$$

for an appropriate value of $\lambda = \text{const.}$

Let us now turn to goal-seeking procedures or to the application of reference points and their local utility fields. We could interpret the result in Figure 9 in another way. Let us choose on every curve $g(\lambda, \tilde{Q})$ an arbitrary reference point whether it is feasible or not. There we can consider every field of indifference curves (left lower angles in Figure 9) as preference levels of the reference points on this curve. The corresponding efficient point is obtained by maximizing the preference levels related to a chosen reference point.

The disadvantage of this interpretation is that the reference point only plays a formal role because the field levels do not depend on the distance of the field curves from the reference point. However, reference points can represent the important wishes of the decision maker. Thus it would be very useful to give the reference points an essential influence on the seeking process for efficient points. This can be done simply by introducing local fields of preference levels that express how far we are from reaching our aims.

We first represent local preference level fields for Pareto optimality and then introduce for the first time the notion of direction diagrams. We introduce a symmetrical field of Pareto preference level lines as shown in Figure 10. The preference levels show us a certain directional behavior which can be combined with any scalarization depending on the distance r from the reference point. This r -dependent scalarization is not specific for Pareto optimality; it already reflects the local utility of the decision maker in the neighborhood of the reference point under consideration.

We give all zero level points the indifference value 0. The scalarization $f(r)$ should be chosen differently for the worse and better classes. Thus we need two scalarization functions $f_b(r)$ and $f_w(r)$.

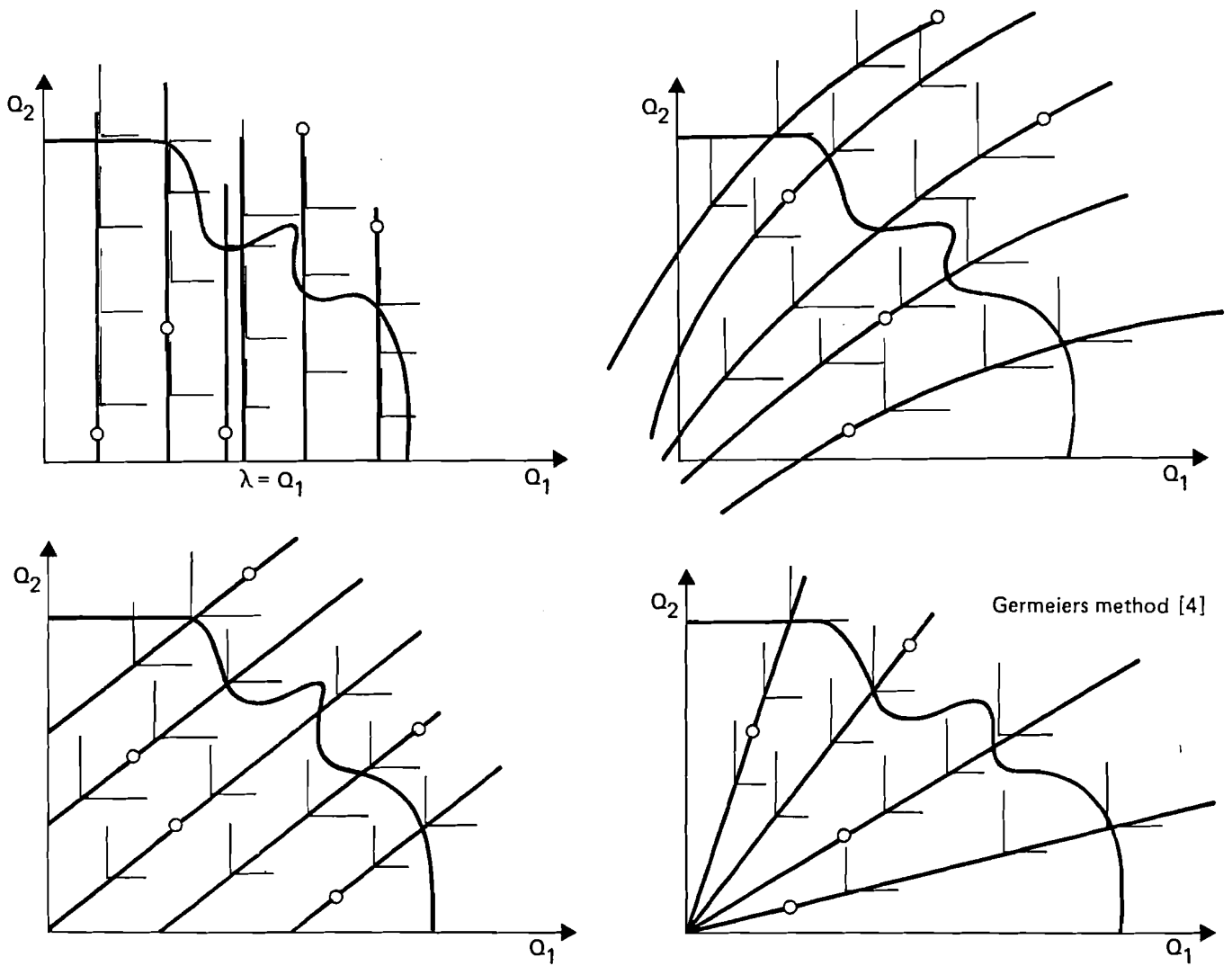


Figure 9: Possibilities to introduce different sets of global compromise criteria

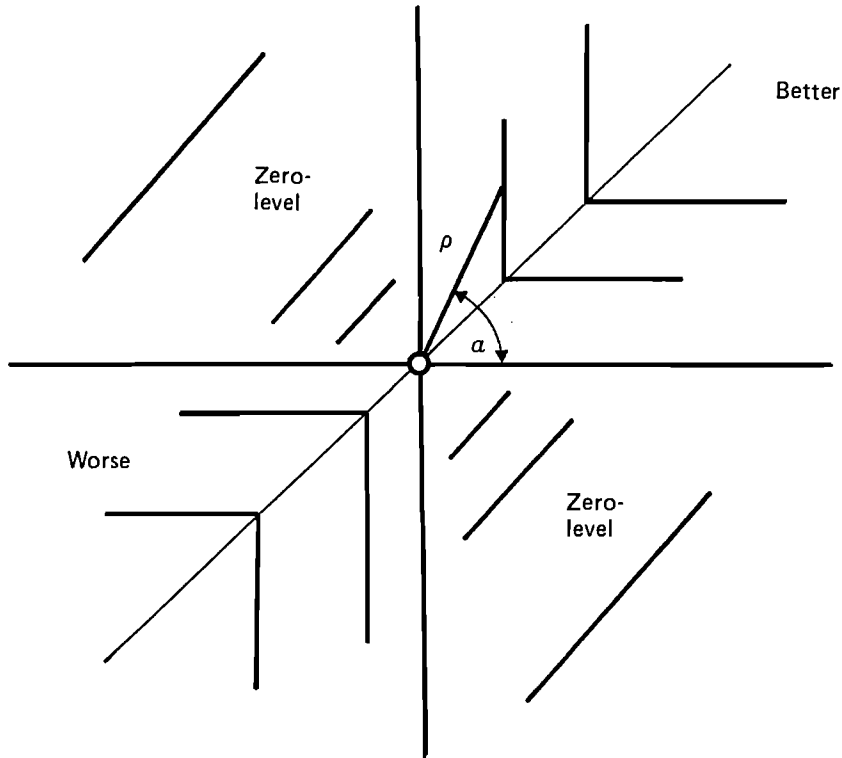


Figure 10: Direction diagram in Pareto-optimality

The model $(f_w(r), f_b(r))$ formalizes the wishes of the decision maker in the neighborhood of the reference point.

As an example, let us consider one concrete case. We want to reach a reference point coming out of "worse", having already achieved a point in "better", to pass to points which are better still. These wishes can be represented by demanding that:

$$f_w(r) \quad ,$$

should be a monotonously decreasing function, and that

$$f_b(r) \quad ,$$

should be a monotonously increasing function. For example,

$$f_w(r) = -r^k \quad ,$$

$$f_b(r) = r^\ell \quad ,$$

k, l are measures of the strength of drift into $r = 0$ or from $r = 0$. Now we try to describe the preference isolines in Figure 10 in polar coordinates (ρ, α) :

$$\alpha = 45^\circ + \Delta, \quad \Delta \geq 0 \quad \rho \cos \alpha = r \cos 45^\circ$$

$$\alpha = 45^\circ - \Delta, \quad \Delta \geq 0 \quad \rho \sin \alpha = r \sin 45^\circ$$

$$0 \leq \Delta \leq 45^\circ.$$

This leads to a uniform description

$$r = \rho(\cos|\Delta| - \sin|\Delta|) \quad -45^\circ \leq \Delta \leq 45^\circ.$$

For the utility or local compromise criterion we get

$$\tilde{Q} = \begin{cases} \rho^l (\cos|\Delta| - \sin|\Delta|)^l & Q \in \text{better} \\ 0 & Q \in \text{indifferent} \\ -\rho^k (\cos|\Delta'| - \sin|\Delta'|)^k & Q \in \text{worse} \end{cases}.$$

The direction diagram for a local utility field does not take into account the ρ dependence and corresponding scalarization but uses only the angle dependency, i.e., it considers the utility variation on the unit circle.

Therefore Pareto optimality is characterized by the direction diagram

$$D = \begin{cases} (\cos|\Delta| - \sin|\Delta|) & -45^\circ \leq \Delta \leq 45^\circ \\ & \text{better} \\ 0 & \text{indifferent} \\ (\cos|\Delta'| - \sin|\Delta'|) & -45^\circ \leq \Delta' \leq 45^\circ \\ & \text{worse} \end{cases}.$$

CONSTRUCTION OF LOCAL UTILITY FIELDS BY DIRECTION DIAGRAMS

Local utility fields are described here as a stepwise decomposition of distance and angle influence by

$$\tilde{Q}(\rho, \alpha) = f_i(\rho) \psi_i(\alpha) \quad i \in D^i$$

$$D^1 \cup D^2 \cup \dots \cup D^k = \text{whole space}$$

$$D^i \cap D^j = \emptyset$$

$$D^i \text{ cones } .$$

This means that we assume a cone decomposition of the whole neighborhood of a reference point and allow that on each component cone D^i the field can be defined in a different way that reflects the imagination of a decision maker.

We normalize $f_i(1) \equiv 1$ and demand that all functions $f_i(\rho)$ are strictly monotonous. We further demand $\psi_i(\alpha) \geq 0$ by introducing any sign into the factors $f_i(\rho)$. The corresponding direction diagram of the local utility field is then

$$D(\alpha) = \psi_i(\alpha) , i \in D^i \quad i = 1, 2, \dots, k .$$

Obviously the roots α^* with

$$D(\alpha^*) = 0 ,$$

are important because they lead to the asymptotes of the preference lines. Now we study some special cases of local fields.

Hyperbolic preference

The fact that the lower left angles L in Pareto optimality are no-indifference lines is unfavorable, because it can lead to catastrophe-like switching properties, as demonstrated in Figure 11.

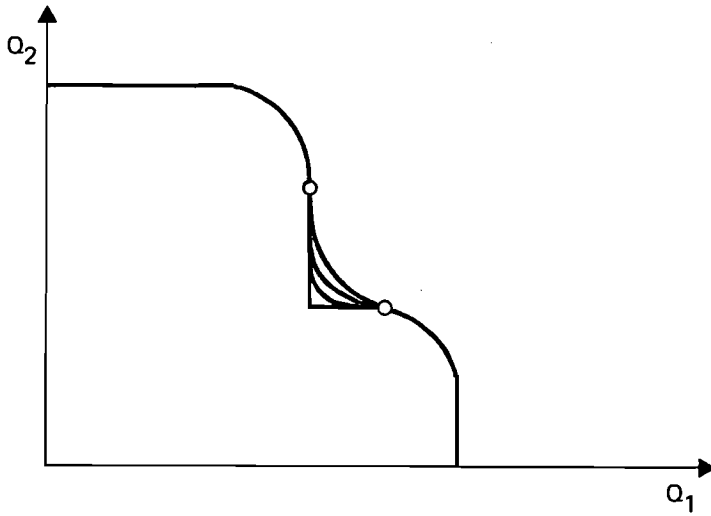


Figure 11: Catastrophe properties of Pareto-optimality

With only a small variation of the constraints, all efficient points on P_1P_2 can switch to either P_1 or P_2 . To eliminate unwanted properties of this kind we introduce preference curves that are hyperbolic in form as shown in Figure 12 instead of left lower angles.

The lines of the field are given by

$$(Q_1 - \tilde{Q})(Q_2 - \tilde{Q}) = K \quad ,$$

with fixed value of K . Obviously for $K \rightarrow 0$ we obtain an approximation of the Pareto preference lines. For the utility values we get the following expression:

$$\begin{aligned} \tilde{Q} &= \frac{Q_1 + Q_2}{2} - \left[K + \left(\frac{Q_1 - Q_2}{2} \right)^2 \right]^{1/2} , & (Q_1, Q_2) \in \text{better} \\ \tilde{Q} &= \frac{Q_1 + Q_2}{2} + \left[K + \left(\frac{Q_1 - Q_2}{2} \right)^2 \right]^{1/2} & (Q_1, Q_2) \in \text{worse} . \end{aligned}$$

This is very similar to Pareto optimality, but with fixed K it has no direction diagram representation.

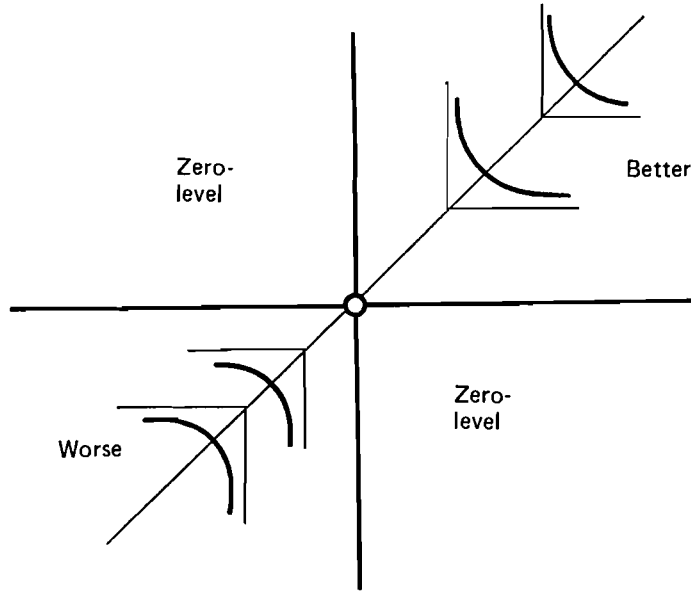


Figure 12: Modification of Pareto-optimality by a set of parallel hyperbola

However, if we put

$$K = \kappa \tilde{Q}^2 ,$$

with $\kappa > 0$, arbitrarily, we get a small deviation from Pareto preference lines for $\tilde{Q} \rightarrow 0$ and an increasing deviation for $\tilde{Q} \rightarrow \infty$. The utility function is now

$$\tilde{Q} = \frac{-Q_1 + Q_2}{2(\kappa - 1)} + \left[\left(\frac{Q_1 + Q_2}{2(\kappa - 1)} \right)^2 + \frac{Q_1 Q_2}{(\kappa - 1)} \right]^{1/2} , \quad Q_1, Q_2 \in \text{better}$$

$$\tilde{Q} = \frac{Q_1 + Q_2}{2(\kappa - 1)} - \left[\left(\frac{Q_1 + Q_2}{2(\kappa - 1)} \right)^2 + \frac{Q_1 Q_2}{(\kappa - 1)} \right]^{1/2} , \quad Q_1, Q_2 \in \text{worse}$$

for $\kappa > 1$. For $\kappa < 1$ the sign of the root must be changed. If we now put

$$Q_1 = \rho \cos \alpha ,$$

$$Q_2 = \rho \sin \alpha ,$$

we get corresponding direction diagrams

$$D = D(\alpha) = \begin{cases} \frac{-\cos \alpha + \sin \alpha}{2(\kappa-1)} + \left[\frac{(\cos \alpha + \sin \alpha)^2}{4(\kappa-1)^2} + \frac{\cos \alpha \sin \alpha}{(\kappa-1)} \right]^{1/2} \\ \frac{-\cos \alpha + \sin \alpha}{2(\kappa-1)} - \left[\frac{(\cos \alpha + \sin \alpha)^2}{4(\kappa-1)^2} + \frac{\cos \alpha \sin \alpha}{(\kappa-1)} \right]^{1/2} \end{cases}$$

We get a more remarkable deviation from Pareto-optimality by using not translated hyperbola as preference lines but

$$Q_1 Q_2 = \tilde{Q} ,$$

which means K itself shall be the compromise objective, see Figure 13. Obviously in this case we have

$$\tilde{Q} = \rho^2 \cos \alpha \sin \alpha .$$

This produces the following direction diagram

$$D = D(\alpha) = \begin{cases} (\cos^2 \Delta - \sin^2 \Delta) & -45^\circ \leq \Delta \leq 45^\circ \\ & \text{better} \\ 0 & \text{indifferent} \\ (\cos^2 \Delta' - \sin^2 \Delta') & -45^\circ \leq \Delta' \leq 45^\circ \\ & \text{worse} \end{cases}$$

This is very similar to the direction diagram of Pareto optimality.

Direction Diagram for Penalty Scalarization Approach (Wierzbicki et al. [3])

We start with an arbitrary cone D spanned by the linearly independent vectors e_1, e_2 . All directions

$$e = \lambda_1 e_1 + \lambda_2 \quad \lambda_i \geq 0 \quad ,$$

belong to this cone.

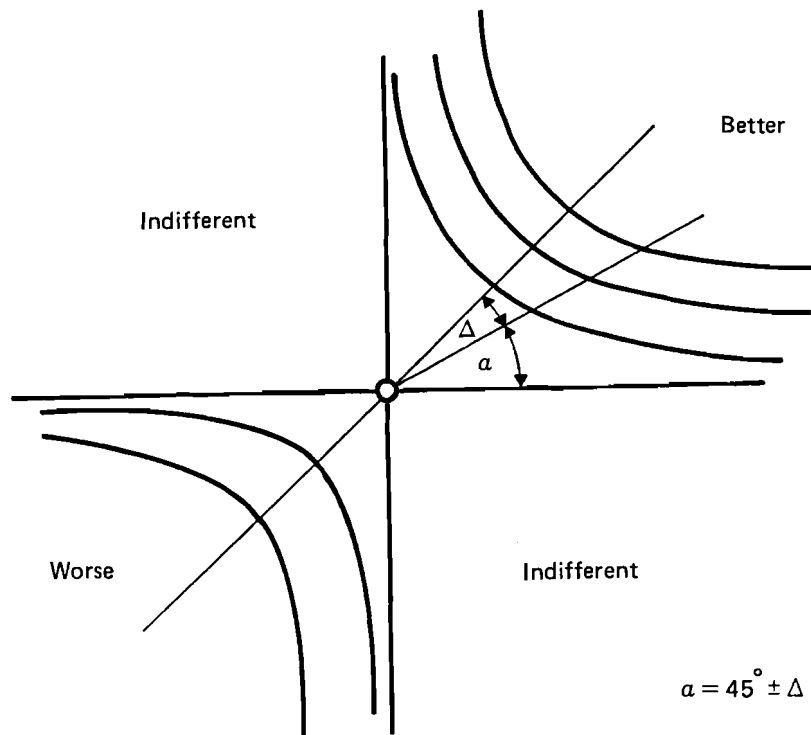


Figure 13: Modification of Pareto-optimality by a set of hyperbola

We then construct the dual cone D^+ on the basis of the dual base (f_1, f_2) corresponding to (e_1, e_2) , which is given by

$$f_1 = (e_2, e_2)e_1 - (e_1, e_2)e_2$$

$$f_2 = -(e_1, e_2)e_1 + (e_2, e_1)e_2$$

$$(f_1, e_1) = (f_2, e_2) = (e_2, e_2)(e_1, e_1) - (e_1, e_2)^2 = G > 0$$

$$f = \eta_1 f_1 + \eta_2 f_2 \quad \eta_i \geq 0 \quad ,$$

f then spans the dual cone D^+ . $Q = (Q_1, Q_2)$ is the objective vector relative to the reference point.

Then the utility function, after the penalty scalarization concept, is given by

$$\tilde{Q} = -\|Q\|^2 + \rho \|P_{D^+} Q\|^2$$

$\rho > 1$ and $P_{D^+} Q$ is the projection of Q on the cone D^+ .

Let us now find the direction diagram representation for this case. From Figure 14 we obtain the following information.

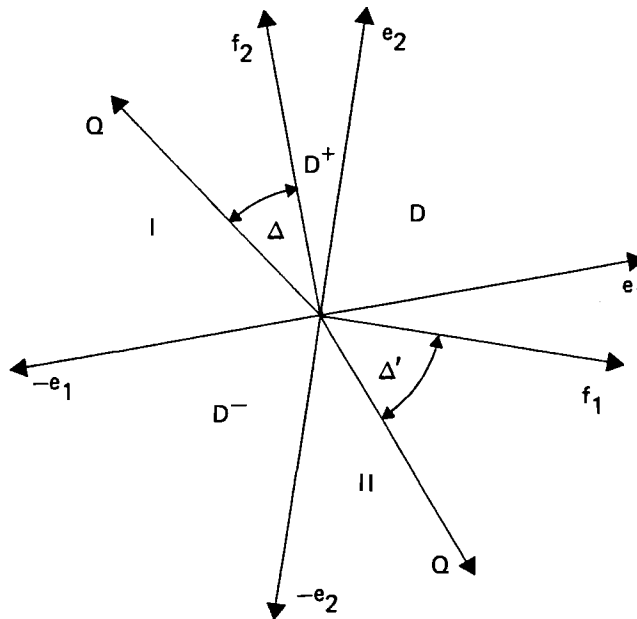


Figure 14: Scheme of preference cones used in the penalty scalarization method

The whole neighborhood of the reference point is obviously decomposed into the four cones D^+ , I, II and D^- . The angles Δ, Δ' ($0 \leq \Delta, \Delta' \leq 90^\circ$) are introduced as shown in Figure 14. Thus for

$$Q \in D^+ \rightarrow P_{D^+} Q = Q$$

$$Q \in I \rightarrow P_{D^+} Q = \frac{(Q, \bar{f}_2)}{(\bar{f}_2, \bar{f}_2)} \bar{f}_2 = \cos \Delta \|Q\| \bar{f}_2 / \|\bar{f}_2\|$$

$$Q \in II \rightarrow P_{D^+} Q = \frac{(Q, \bar{f}_1)}{(\bar{f}_1, \bar{f}_1)} \bar{f}_1 = \cos \Delta' \|Q\| \bar{f}_1 / \|\bar{f}_1\|$$

$$Q \in D^- \rightarrow P_{D^+} Q = 0$$

Therefore we obtain the following result for the penalty scalarization function:

$$\tilde{Q} = \begin{cases} (p-1) \|Q\|^2 & Q \in D^+ \\ \|Q\|^2 (-1 + p \cos^2 \Delta) & Q \in I \\ \|Q\|^2 (-1 + p \cos^2 \Delta') & Q \in II \\ -\|Q\|^2 & Q \in D^- \end{cases}$$

If we maximize the local utility coming from worse D^- we drift to the reference point. Having passed it, which means being already in D^+ , we go in the direction of better and better points. This local utility function has the following directions diagram:

$$D = D(\alpha) = \begin{cases} 1 & Q \in D^+ \\ + \left| \frac{\rho \cos^2 \Delta - 1}{\rho - 1} \right| & Q \in I \\ \left| \frac{\rho \cos^2 \Delta' - 1}{\rho - 1} \right| & Q \in II \\ + \frac{1}{\rho - 1} & Q \in D^- \end{cases}$$

$\rho - 1$ is a drift factor. This representation is not very convenient; it seems better to choose those cones whose sides are asymptotes of the direction diagram. Taking this into account we obtain a decomposition into only two cones bounded by straight lines defined by

$$\begin{aligned} \Delta_0 \quad \text{with} \quad \cos^2 \Delta_0 &= \frac{1}{\rho} \quad \sim \quad \Delta_0 = \Delta'_0 \\ \Delta'_0 \quad \text{with} \quad \cos^2 \Delta'_0 &= \frac{1}{\rho} \end{aligned}$$

Figure 15 shows the result qualitatively. Obviously the behavior of this approach in D^+ and D^- is similar to that proposed by Salukvadse [5].

This is a notable difference to Pareto optimality: we now have not an indifference area, but a curve. Obviously this behavior is good for a vector minimum problem, because with high velocity (~ 1) we are approaching the reference point from the "northeast", and leave it to the "southwest" with a lower velocity ($\frac{1}{(\rho-1)}$). For a vector maximum problem the role of "northeast" and "southwest" cones should be interchanged. This could be done by a penalty scalarization function of the form

$$\tilde{Q} = \|Q\|^2 - \rho \|Q - P_{D^+} Q\|^2,$$

leading to the direction diagram

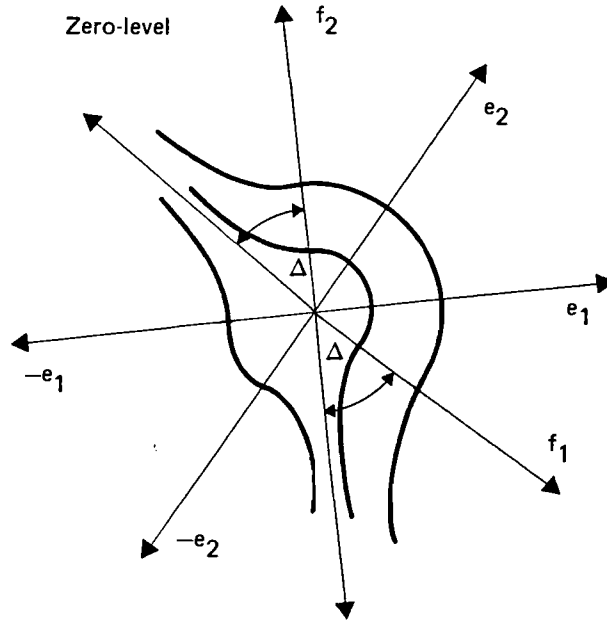


Figure 15: The indifference lines in the penalty scalarization method

$$D = D(\alpha) = \begin{cases} \frac{1}{\rho-1} & Q \in D^+ \\ \left| \frac{\rho \sin^2 \Delta - 1}{\rho-1} \right| & Q \in I \\ \left| \frac{\rho \sin^2 \Delta' - 1}{\rho-1} \right| & Q \in II \\ 1 & Q \in D^- \end{cases} .$$

THE RELEVANCE OF LOCAL UTILITY FIELDS FOR FINDING EFFICIENT POINTS

It seems quite natural that the decision maker expresses his goals in the language of local utility fields in the objective space. In the seeking process for efficient points this is confronted with the real possibilities and thus he gets a proposed point as a compromise between his goals and reality.

However we think that for decision makers who are themselves analyzing the relationship between controls a and objectives Q it should be useful to formulate local utility fields on the control space, taking into account a priori experience from past seeking steps and goals expressed in control terms. Particularly in technical engineering are people able to express what is good and what is bad in terms of control variables. The direction diagram method exposes two features of local utility fields:

- (1) reward or punishment of directions (leading or leaving a reference point);
- (2) evaluation of the distance r from the reference point independently from the direction.

The reward of directions is formalized by the direction diagram

$$D = D(\alpha) \geq 0, \quad D_{\max} = 1,$$

which is often decomposed into

$$D(\alpha) = \psi_i(\alpha), \quad \alpha \in I_i = (\alpha_i, \alpha_{i+1}),$$

where α_i is a root $D(\alpha_i) = 0$ or a first-order discontinuity point

$$D(\alpha_i^+) - D(\alpha_i^-) \neq 0.$$

In the inner points of I_i the components $\psi_i(\alpha)$ should be continuous functions. For discontinuity points we put

$$D(\alpha_i) = \frac{1}{2} \left(D(\alpha_i^+) + D(\alpha_i^-) \right).$$

It is possible to express good imagination of a decision maker in the language of direction diagrams.

Let us give some examples:

- (1) The decision maker is already at a reference point and wants to leave it into the angle "better" with high velocity.

The corresponding local utility field could be

$$\tilde{Q} = \begin{cases} K \|Q\|^2 & Q \in D^+ = D \\ 0 & \text{else} \end{cases},$$

as shown in Figure 16. This goal belongs to approaching efficient points with a "cooperative strategy". The more we approach efficient points the more difficult it will be to succeed with cooperative steps. Now "contradictory" steps become more and more important. This means we first apply direction diagrams, taking into account indifferent points, and after some time the indifferent points should increase in weight. Figure 17 shows an intermediate stage and Figure 18 a stage in the neighborhood of efficient points. These figures reflect an ideology which is good if we have already reached the reference point; they should be combined with the monotonously increasing radius function $f(r)$ or $f_i(r)$; for example, $f_i(r) \sim r^2$ (Salukvadse-ideology).

However, if the reference point is a goal (feasible or not) we need a corresponding direction diagram for the landing. If we assume that the goal is feasible and not efficient, we could try with "cooperative" landing using the direction diagram of Figure 19. The nearer the goal lies to efficient points the more we should use the possibilities of landing from contradictionally points, as shown in Figures 20 and 21.

If we want to reach the goal reference points and to go further we have only to superpose the "landing" and "starting" fields with different weights.

Let us now study how this thinking could be expressed in the control space. First let us remark that this kind of thinking is not new but has been used formerly in stochastic seeking procedures of monetary optimization (see for example [6]). If we have only a single objective Q , we can write

$$Q = f(a_1, a_2, \dots, a_k) \quad .$$

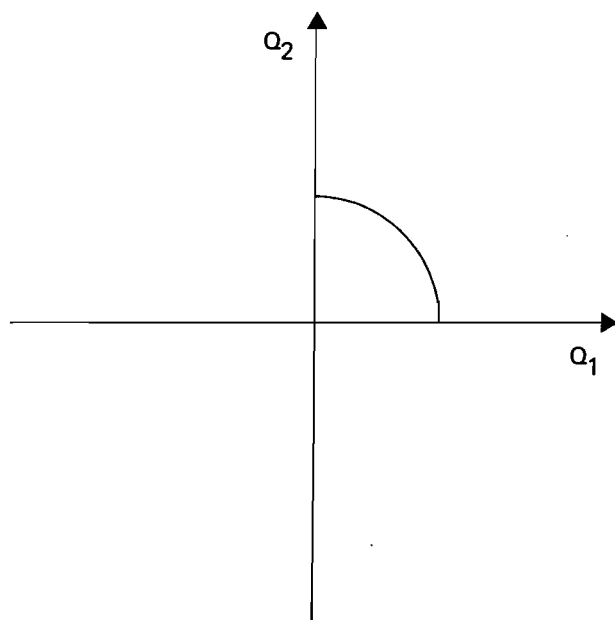


Figure 16: A direction diagram in an initial point far from efficiency

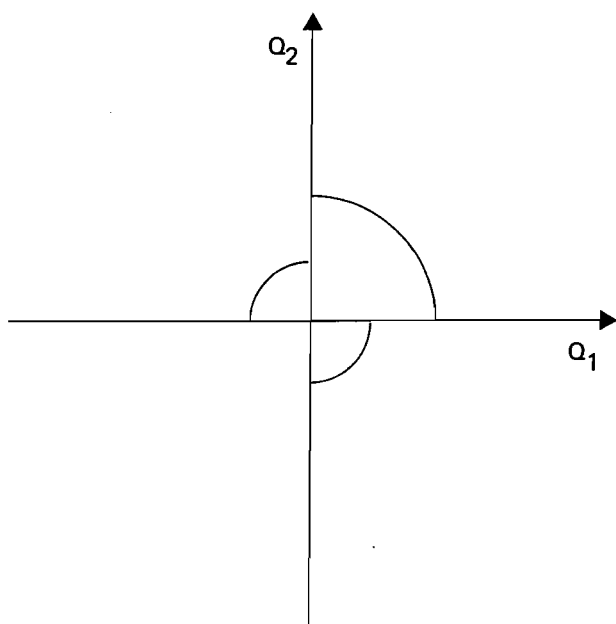


Figure 17: A direction diagram in an initial point in medium distance from efficiency

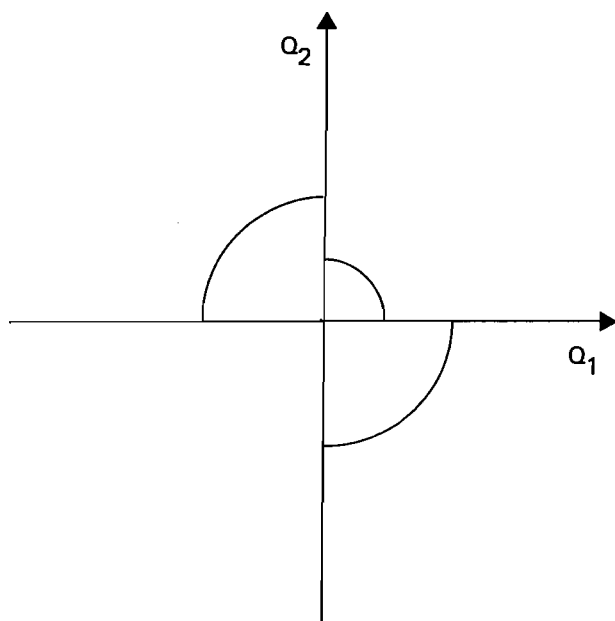


Figure 18: A direction diagram in an initial point in the neighborhood of the efficient set

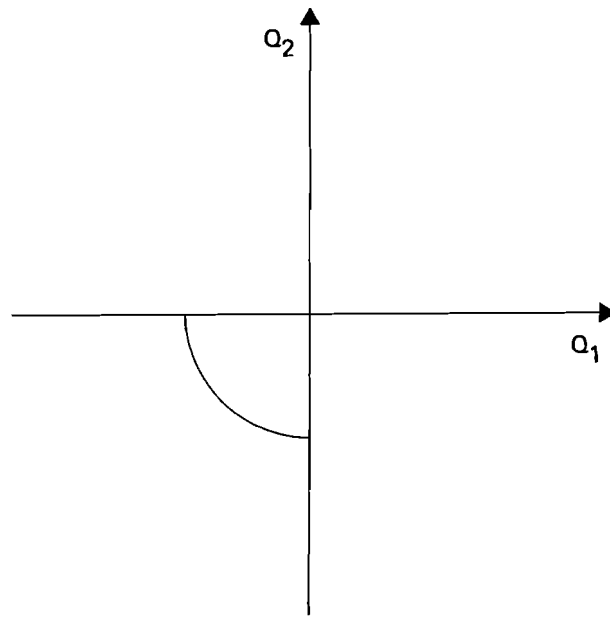


Figure 19: A direction diagram in a goal point far from efficiency

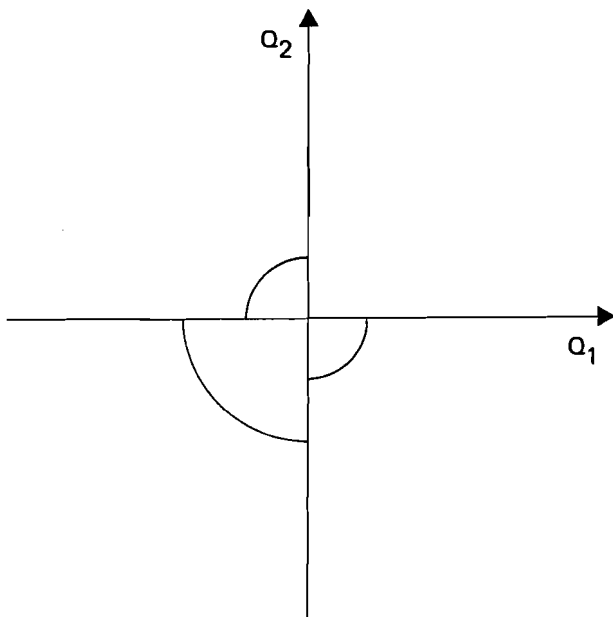


Figure 20: A direction diagram in a medium distance from the efficient set

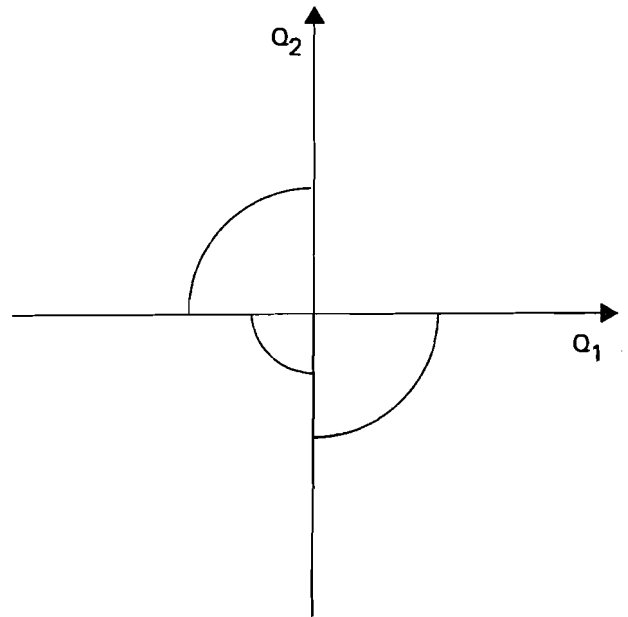


Figure 21: A direction diagram in a goal point near the efficient set

Having done a seeking step from a to a' and being successful we like to reward the corresponding direction distinctly, or to reward more or less all directions of the corresponding half-space. Sometimes we also give a certain chance to the opposite direction. Figures 22 to 25 show corresponding direction diagrams.

Some years ago we interpreted these direction diagrams as probability densities of directions and got highly efficient stochastic seeking procedures from this kind of thinking.

Now we interpret the different direction diagram models for the design of the next seeking step, then the coordinates Q_1 and Q_2 should be substituted by their corresponding gradient vectors $e_1 = \text{grad } Q_1$ and $e_2 = \text{grad } Q_2$. But the cone "better" is not spanned by e_1, e_2 but by the corresponding dual base

$$f_1 = (e_2, e_2)e_1 - (e_1, e_2)e_2 \quad ,$$

$$f_2 = -(e_1, e_2)e_1 + (e_1, e_1)e_2 \quad .$$

This means the Pareto cone decomposition from the objective space is transformed into the cone decomposition shown in Figure 26.

Starting from an initial point far from efficiency we should by analogy with Figure 16, use a direction diagram as shown in Figure 27. After some time and taking into account the larger angle between the gradients, we are already using contradictory steps obtained from the direction diagram in Figure 28 by analogy with Figure 17. If we come nearer to efficient points the angles between gradients usually approach π and then we should stress more and more the contradictory directions using the direction diagram of Figure 29 by analogy with Figure 18.

This tendency to switch between different forms of the direction diagrams is automatically realized in approved seeking procedures. Let us show how this is done in the antiparallel gradient method (Ester [3]).

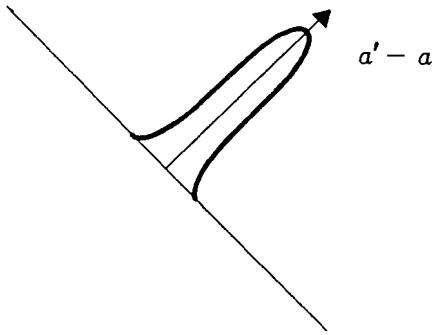


Figure 22: Reward of a direction

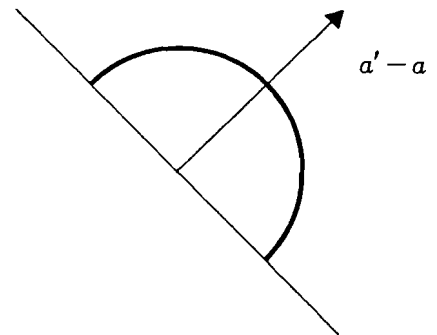


Figure 23: Uniform reward of a half-space

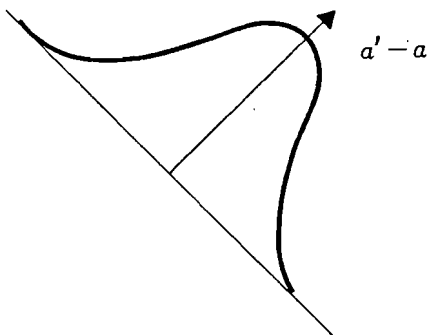


Figure 24: Reward of a half-space by a forward direction diagram

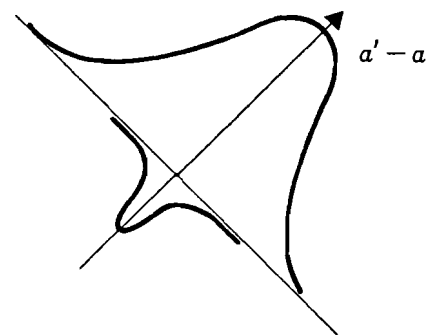


Figure 25: Reward of a half-space by a forward direction diagram with a little back-looking

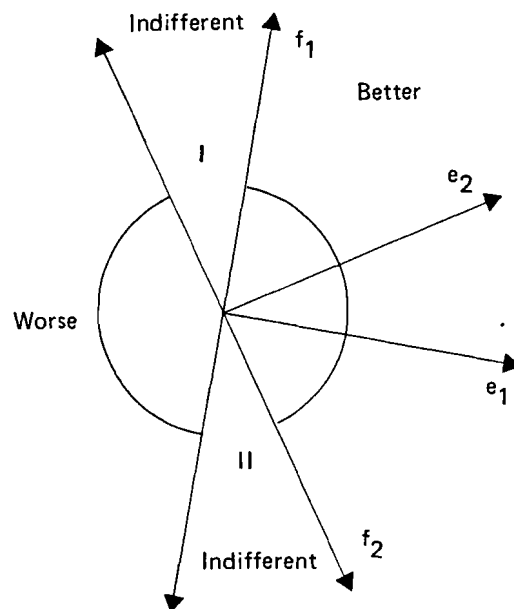


Figure 26: Cone-structure in the control space using information from the gradient-directions

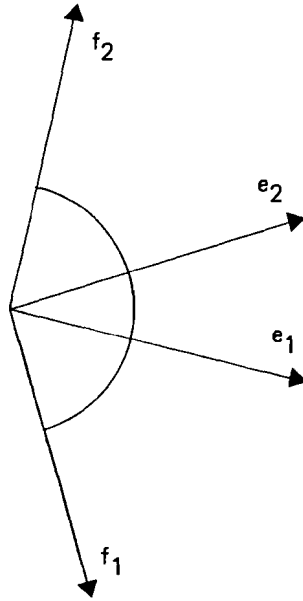


Figure 27: Direction diagram in control space in an initial point far from efficiency

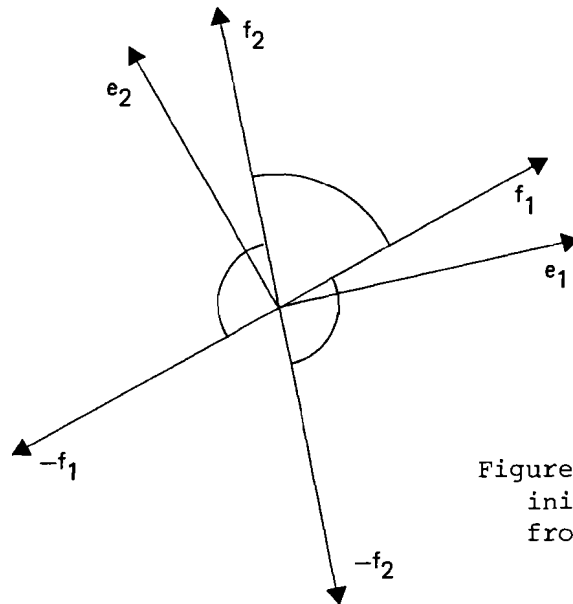


Figure 28: Direction diagram in an initial point with medium distance from the efficient set

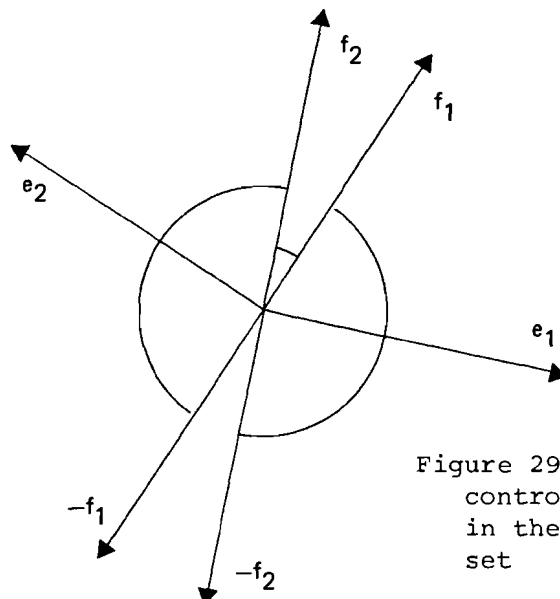


Figure 29: Direction diagram in control space in an initial point in the neighborhood of the efficient set

This proposes a step of the following form

$$\Delta a = k \left(\frac{e_1}{\|e_1\|} + \rho \frac{e_2}{\|e_2\|} \right) , \quad 0 \leq \rho ,$$

ρ exposes (for $\rho > 1$) a tendency for the selfish optimum of Q_2 .

Between the base (e_1, e_2) and the corresponding dual base (f_1, f_2) , we have the following transformations:

$$f_1 = (e_2, e_2)e_1 - (e_1, e_2)e_2 , \quad e_1 = (f_2, f_2)f_1 - (f_1, f_2)f_2 ,$$

$$f_2 = -(e_1, e_2)e_1 + (e_1, e_2)e_2 , \quad e_2 = -(f_1, f_2)f_1 + (f_1, f_1)f_2 ,$$

with

$$G_e = (e_1, e_1)(e_2, e_2) - (e_1, e_2)^2 = \frac{1}{G_f} = \frac{1}{(f_1, f_1)(f_2, f_2) - (f_1, f_2)^2}$$

$$(f_i, f_h) = \frac{(e_i, e_j)}{G_e} , \quad (e_i, e_j) = \frac{(f_i, f_j)}{G_f} .$$

If we express the step in the dual base (f_1, f_2) we get the following representation:

$$\Delta a = \|f_2\|^3 \|f_1\| \sin \alpha' \left[(1 - \kappa \cos \alpha') \frac{f_1}{\|f_1\|^2} + (\kappa - \cos \alpha') \frac{f_2}{\|f_2\|} \right]$$

with

$$\kappa = \rho \frac{\|f_1\|^2}{\|f_2\|^2} , \quad \alpha' = \pi - \alpha , \quad \cos \alpha = \frac{(e_1, e_2)}{\|e_1\| \|e_2\|} .$$

In the antiparallel gradient method, $\rho > 1$ is chosen. However, for variable κ : $0 \leq \kappa \leq 1$, we will discuss the step in terms of a direction diagram without evaluating it explicitly.

$$(1) \quad 0 \leq \alpha \leq 90^\circ \rightarrow \alpha' > 90^\circ$$

$$\rightarrow 1 - \kappa \cos \alpha' > 0$$

$$\kappa - \cos \alpha' > 0$$

we obtain a diagram only in D^+ . This means that we look for a cooperative step.

$$(2) \quad \alpha > 90^\circ \rightarrow 0 \leq \alpha' \leq 90^\circ$$

For $\cos \alpha' < \kappa < \frac{1}{\cos \alpha'} \rightarrow \text{step in } D^+$

$\alpha' \rightarrow 0$, this interval becomes smaller and smaller.

$$\kappa > \frac{1}{\cos \alpha'} \geq 1 \rightarrow \kappa - \cos \alpha' > 0 \rightarrow \text{step in II,}$$

$$\kappa < \cos \alpha' \leq 1 \rightarrow 1 - \kappa \cos \alpha' > 0 \rightarrow \text{step in I.}$$

This occurs more and more, if $\alpha \rightarrow \pi$.

No step will be done into D^- .

It is useful to interpret the antiparallel gradient method in terms of local utility fields. To superpose the interests of Q_1 and Q_2 means the interaction of selfish local utility fields each for the benefit of these criteria.

If we stay within the neighborhood of a reference point where linear models are valid we get two local utility fields

$$\Delta Q_i = (\text{grad } Q_i, \Delta a) \quad , \quad i = 1, 2 \quad .$$

The corresponding levels are straight lines parallel to the dual vectors f_i as shown in Figure 30. We see in "better" cooperative interests, in I and II competitive interests of both criteria. The direction diagram should be a compromise between this knowledge and the local goals of the decision maker.

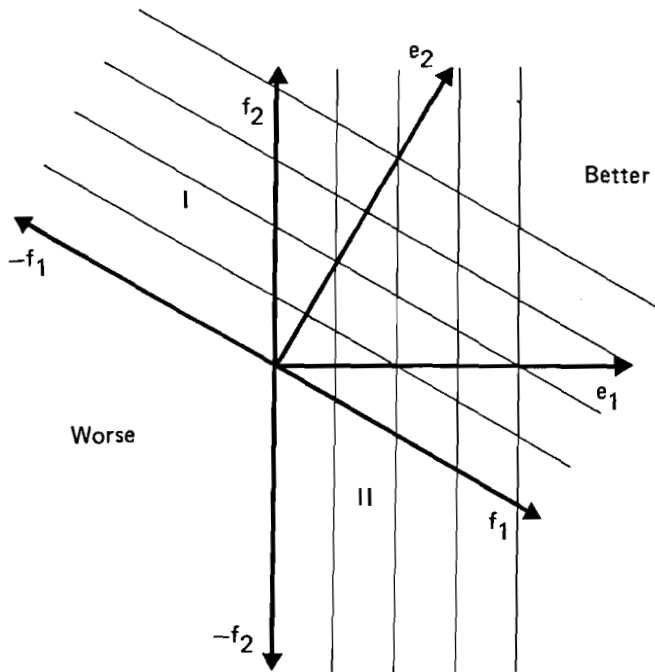


Figure 30: Local utility fields using the linear models for both objectives

Obviously in an antiparallel gradient method the compromise local utility field consists of straight lines parallel to the axis e_2 . We distinguish two cases: $0 \leq \alpha \leq \frac{\pi}{2}$, Figure 31, and $\frac{\pi}{2} < \alpha \leq \pi$, Figure 32.

We see, for $0 \leq \alpha \leq \frac{\pi}{2}$ and $\kappa > 0$ that all steps are cooperative ones not exhausting all cooperative possibilities. For $\kappa < 0$ we would first get additional indifferent steps for the benefit of Q_1 and afterward even worse steps. In $\frac{\pi}{2} < \alpha \leq \pi$ and $\kappa > 0$ we get cooperative steps, for small κ indifferent steps for the benefit of Q_1 and for large κ indifferent steps for the benefit of Q_2 , not all indifferent possibilities being exhausted. For $\kappa < 0$ we would only get more indifferent steps for the benefit of Q_1 .

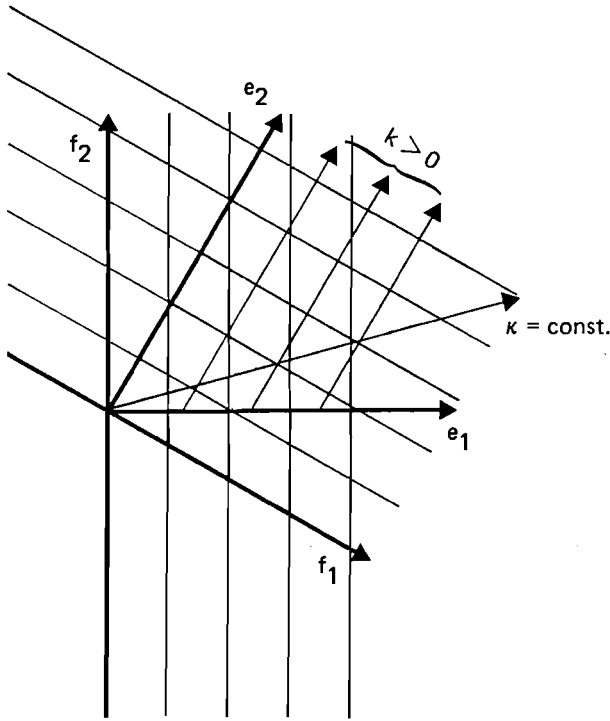


Figure 31: Local utility field for the antiparallel gradient method with a small angle ($0 \leq \alpha \leq 90^\circ$) between the gradients

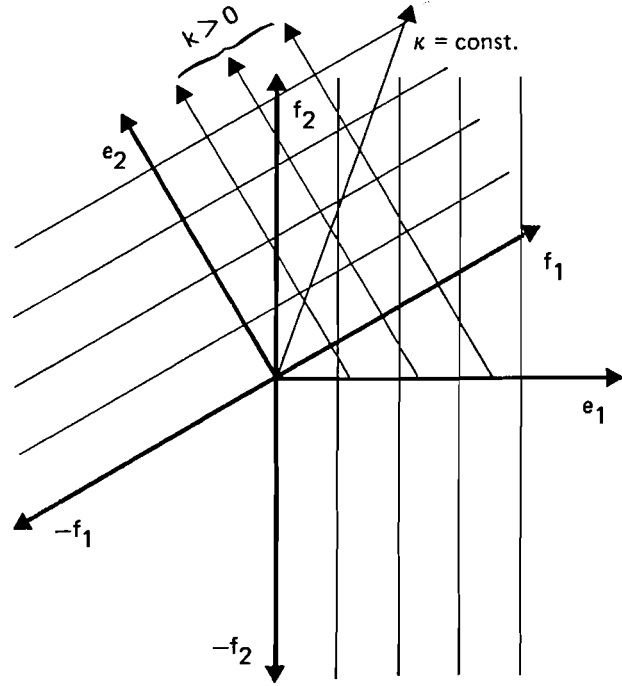


Figure 32: Local utility field for the antiparallel gradient method with a large angle ($90^\circ < \alpha \leq 180^\circ$) between the gradients

CONCLUSION AND QUESTIONS FOR FUTURE RESEARCH

1. There is a strong interrelationship between the notions preference, reference, convexity and efficiency in Pareto optimality in a two-dimensional case. This could be generalized to higher dimensional space but not with a convexity concept based on special curves as generalized straight lines. The generalization of supporting hyperplanes is quite obvious.

2. In the two-dimensional space other curves, for example hyperbola, can be used instead of angles for the definition of an optimality notion. The interrelationship between preference, reference, convexity and efficiency obviously will be very similar to the Pareto case discussed above. It is natural to introduce the preference relation by a local field defined by corresponding direction diagrams. We come to a successful convexity notion only if we refer to a field with a given form to every point of the plane. The question arises, under which conditions for the uniform local field the following field property in the plane will be fulfilled [see [7]]. Every pair

of points P_1, P_2 defines a single sequence $P_1 P_2$ belonging to a curve of the field through these two points for a deduced maximum convexity and another single sequence $P_1 P_2$ for a deduced minimum convexity. Figure 33 illustrates the question. The curves in "better" and II define angles to the left and lead to maximum convexity, whereas the curves in I and "worse" define angles to the right and lead to minimum convexity.

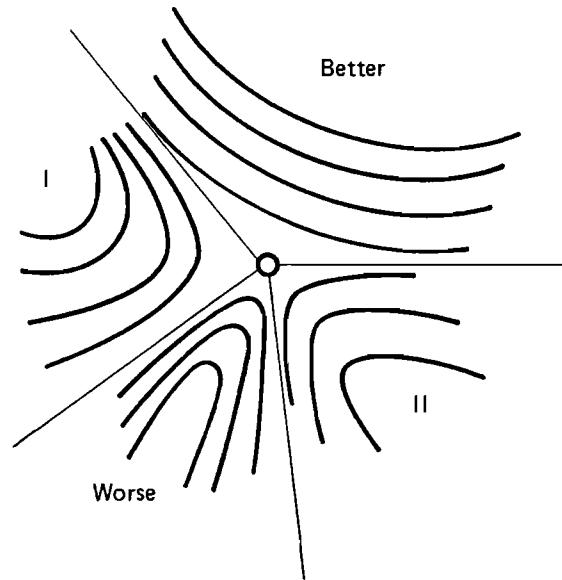


Figure 33: Local curve field for the generation of a generalized maximum and minimum convexity

3. Local utility fields can be interpreted as membership functions for a fuzzy goal, if the reference point is a goal or as membership functions for a fuzzy lower or upper threshold. How do we make use of fuzzy set theory to construct good local fields which help the seeking process for efficient points according to the agreed optimality notion?

4. We have shown how useful information from linear models can be used in control space to construct good goal seeking local utility fields.

The problem is, how can this be done with the possible benefit of larger step-widths if we make use of local quadratic

models instead of linear ones? How will Pareto optimality be represented in control space if we have reliable quadratic models

$$\Delta Q = (\text{grad } Q, \Delta a) + \Delta a^T \left(\frac{\partial^2 Q}{\partial a \partial a'} \right) \Delta a ,$$

in the neighborhood of a reference point?

REFERENCES

- [1] Peschel, M. (1979) Ingenieurtechnische Entscheidungen mit Hilfe der Polyoptimierung. Berlin: VEB Verlag Technik.
- [2] Ester, J. (1975) Dialogverfahren als wichtiges Hilfsmittel zur Lösung mehrkriterieller Optimierungsverfahren. Habilitation, TH Karl-Marx-Stadt.
- [3] Wierzbicki, A. (1977) Basic properties of scalarizing functions for multiobjective optimization. Math. Operationsforsch. Statist., Ser. Optimization 8(1): 55-60.
- [4] Wierzbicki, A. (1979) The Use of Reference Objectives in Multiobjective Optimization--Theoretical Implications and Practical Experience. WP-79-66. Laxenburg, Austria: International Institute for Applied Systems Analysis.
- [5] Salukvadse, M.E. (1974) On the existence of solutions in problems of optimization under vector-valued criteria. Journal of Optimization Theory and Applications, 13(2).
- [6] Peschel, M. (1972) Statistische Modellbildung. Reihe Automatisierungstechnik 137, VEB Verlag Technik, Berlin.
- [7] Peschel, M. (1966) Untersuchungen über den Begriff der Konvexität. Dissertation, Math. nat. Fakultät, Humboldt University, Berlin.